

## Single Phase Heat Transfer In Parallel Micro-Channel Heat Sink

**R.SH.AL-Khafajy**

College of Engineering , Mechanical Engineering Department , Thi-Qar University,Iraq, E-mail: [alraad461@gmail.com](mailto:alraad461@gmail.com)

---

### Abstract

A copper parallel channels test piece has built into the test section containing twenty five, one mm by one mm, parallel channels the channels were fifty mm long; the Heat-transfer coefficients for single-phase are reported. Micro-channel was Square shape and the test section has a glass top plate to permit visual observations. The data are taken while the rig is working .The test section is received the heat by an electric heater is associated normally with a boundary condition for constant heat flux. Because the important variation in the single-phase - heat-transfer coefficient in the inlet zone, the interceding copper and aluminum material is shown to make the test section close isothermal wall boundary condition. The heat conduction influence is taken into computation in the data analysis finally; the effective heat flux and the single-phase heat transfer coefficient are reported in this paper experiments and predictions.

Key words— Single phase Heat transfer coefficients , Parallel channels ,Heat flux,Mass flux.

---

### 1. Introduction

In the early years, electronic devices, such as micro-processors and lasers, have increased in power consuming and decreased in physical size. This has guided to an increasing heat intensity that wants to be eliminated through normal operation. Eliminating heat is becoming increasingly complicate with existing rules and it therefore appears probable that new rules will want to be improved. One probability is to utilize a boiling fluid as the coolant, as this would transfer importantly more heat than its single-phase equivalent. This has guided to a plenty of research into boiling in small diameter channels. A realization study in single-phase micro-channel heat sinks was investigated by [1]. Thereafter, micro-channel heat sinks have extradited large notice by investigators. Single phase flows in micro channel heat sinks have been widely reported [2, 3]. A summarize of investigates have been endeavored for single tubes, e.g. [1, 2]. Several investigates have endeavored to relate the heat-transfer coefficient by developing the macro-scale connections. These accesses divide the heat transfer into nucleate and convective boiling portions. The effects produced are complexes and cannot be utilized with evidences, see, for example, [3] and [4].

The implementation of micro-channels to electronics cooling impels heavy design restrictions on the system design. For a specified heat dispersion rate, the flow rate, pressure drop, fluid temperature rise, and fluid inlet to surface temperature variation demands determine the optimization of the channel geometry. A number of researchers have investigated the geometrical optimization of micro-channel heat exchangers, including [5-9] the results found by Kandlikar and Upadhye. [9] investigated

a micro-channel system. For a chip of length 510 mm and width 510 mm, they reported an analysis scheme for heat transfer and pressure drop by incorporating the entrance region influences. The number of channels was utilized as a parameter in developing the optimization sketch. The maximum chip temperature was set at 360 K whilst the fluid inlet temperature was set equal to 300 K. The channel depth was supposed to be 200  $\mu$ m.

### 2. Operating Conditions

One test was executed to exams the characteristics of single phase heat transfer into the parallel channel copper test piece with R113 as working fluid. The single-phase exams were achieved by supplying R113 fluid flow close to temperature and atmospheric pressure to the test section. One single-phase test was executed on for reporting the single-phase heat transfer coefficients. Four mass flow rates were utilized for each exam series. The operating conditions for single- phase and flow test are defined to base for the exam series as follows.

### 3. Parallel Channel Surface Tests with R113

For the parallel channel, copper test piece; single-phase heat transfer coefficients were obtained for heat loads in the range of 30.5 – 112.1 W , This presented manifest heat fluxes of 12.5 – 44.84 kW/m<sup>2</sup> , relied on the base area of the test piece. Four mass flow rates between 5-11.3 g /s were utilized. This supplied mass fluxes in the range of 200 – 452 kg /m<sup>2</sup>.s , relied on the regulated flow area in the test piece channels. The four mass flow rates utilized in the single-phase heat transfer tests were utilized for each heat flux, Table 1.

**Table 1 : Operating conditions for single- phase tests**

Single – phase Heat Transfer Tests						
Test piece	Working Fluid	Inlet Fluid temp. [°C]	Mass Flow Rate [ g/s ]	Mass flux [kg/m <sup>2</sup> s]	Heat Applied [ W ]	Heat Flux [kW/m <sup>2</sup> ]
Parallel channel	R113	21.588 – 27.093	5.0 – 11.3	200 – 452	30.5 – 112.1	12.5– 44.84

**1. Experimental Procedure**

The flow loop is presented figure (1) schematically. Before to running each single phase flow exam series, the working fluid was degassing by vigorous boiling for closely three hours to force any dissolved gases to run away from the system to the ambient. During this interval the vent valve above the condenser was periodically opened to permit dissolved gases goes to elopement to the atmosphere. This furthermore set the test pressure to close atmospheric. After degassing the liquid, as it was observed that no gas or air bubble coming out of the liquid inside the test piece before to boiling, flow boiling exams were executed. Exams were conducted by setting the wanted liquid mass flow rate and inlet temperature. Mass flow rate was adjusting by the by-pass valve and modify by the throttling valve located before the filters.

The pre-heater was linked to a controller. With respect to the exam’s mass flow rate, the controller was adjusting to the wanted applied heat to the fluid flow which was passing the pre-heater, to supply the required inlet temperature. Simultaneously the test section heater was adjusting to the required heat flux to the test piece. The liquid was distributed through the flow loop until the wanted entry temperature was obtained. This took three hours approximately. Steady state conditions were obtained when the fluid outlet, heater and the aluminum housing temperatures were seen to be stable. This took half an hour approximately. All of the wanted readings were achieved before the heat flux was re-set to the next required value and the process iterated. During the exams to maintain the system pressure close the atmospheric pressure, the vent valve above the condenser was periodically open and a balloon was connected to it to block the vapor to elopement from the system.

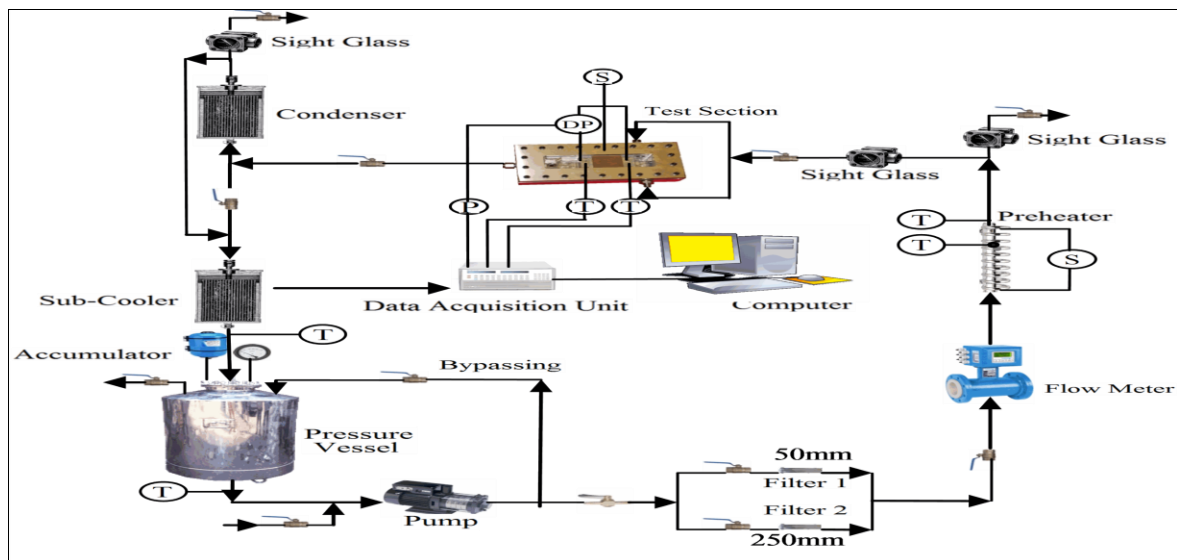


**Fig. 1: Schematic of flow loop[10]**

Fig. 2 .the aluminum test section is shown. Liquid entered the inlet plenum of the test-section through the two inlet ports, set at 90° to the direction of stream in the aluminum test piece. The plenum chamber dimensions were set to reduce the liquid velocity to close to zero before it.

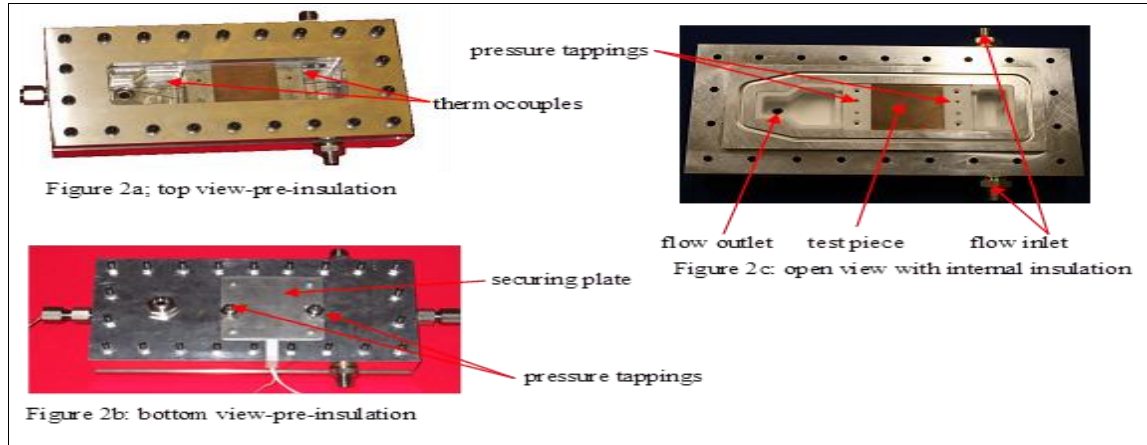


Fig.2. Test section[10]

## 2. Effective heat flux in parallel channel

The heat which is transferred from the heater to the test piece is commensurate with the difference between the test piece surface temperature ( $T_w$ ) and the heater temperature, ( $T_h$ ), .. Data got when the liquid outlet temperature was below the saturation temperature, concluded from the outlet fluid pressure, were utilized to establish this relationship.

$$q_{eff} = 0.4789 (T_h - T_w) - 0.7618 \quad (1)$$

In Which the heat fluxes  $q_{eff}$  unit is in ( $\text{kW/m}^2$ ), and the temperatures' units are in( Kelvin). Equation (1) predicts the heat flux to an accuracy of  $\pm 7\%$  at the lower heat fluxes and  $\pm 1\%$  at the higher values. The constant term guesses the heat loss through the glass window. This corresponds to 2.5 W nearly. At the atmospheric pressure the constant value is reasonable because of the fluid temperature, and the bulk of the test section temperatures were near to the saturation temperature of R113.If the transmission efficiency is given as the ratio of the base heat flux to the heat flux applied by the heater, Eq. (1) produced to transmission efficiencies of 66%–70%, relying on the mass flux.

## 3. Data reduction

The design of the test section comprises two plates placed in between a ceramic heater and R113 fluid. One plate is made from copper and one from aluminum. Each is 50 mm width and 50 mm length and 5 mm in thickness. During single-phase flow the sensible heat gain by the liquid is given by:

$$q_{sp} = M C_p (T_{out} - T_{in}) \quad (2)$$

Where  $q_{sp}$  single-phase heat transfer in ( $\text{kW/m}^2$ ), M mass flow rate ( $\text{kg/s}$ ),  $C_p$  specific heat capacity ( $\text{J/kg}\cdot\text{K}$ ),  $T_{in}$  is inlet fluid temperature (K) and  $T_{out}$  is outlet fluid temperature( K). At the beginning, a uniform heat flux was found for ( $q_b$ ). This permitted the local outlet and inlet heat-transfer coefficients to be got from a one-dimensional heat balance through a small flow length ( $\Delta z$ ) at the base of the channel gave [11]:

$$q_b (W_{ch} + W_w) = \alpha \Delta T_{LMTD} [W_{ch} + 2\eta H_{ch}] \quad (3)$$

The log mean temperature difference (LMTD) represents the wall to fluid temperature difference [11]:

$$\Delta T_{LMTD} = \frac{T_{out} - T_{in}}{\ln\left(\frac{T_w - T_{in}}{T_w - T_{out}}\right)} \quad (4)$$

Where  $T_w$  presents the average wall temperature (K). In which  $q_b$  is the local base heat flux,  $\alpha$  is the single-phase heat-transfer coefficient,  $\eta$  is the fin efficiency,  $H_{ch}$  is the height of the channel,  $W_w$  is the width of the channel wall,  $W_{ch}$  is the channel width and the local wall temperature,  $T_w$  for single phase flows. The size of the heights and widths in Equation (3) are given in Table (2). The fin efficiency was determined by considering that the fins could be processed as rectangular fins with adiabatic tips, i.e.

$$\eta = \frac{\tanh(\lambda H_{ch})}{\lambda H_{ch}} \quad (5)$$

In which  $\lambda$  was the fin parameter, which is given by

$$\lambda = \sqrt{\frac{2\alpha}{k_c W_w}} \quad (6)$$

Where  $k_c$ , is the thermal conductivity of copper and  $\alpha$  single-phase heat transfer coefficient. An initial analysis revealed that the fin efficiency was always near to unity. It was subsequently got as one. The copper test piece has three thermocouples 12.5 mm from the inlet was set inside and also three thermocouples 12.5 mm from the outlet was set inside the copper test piece. In total, there are six thermocouples in the copper test piece, hereafter indicated to as the inlet and outlet locations. The alteration in the measured outlet and inlet wall temperatures was normally less than  $0.6^\circ\text{C}$ , but could, on occasion, be as large as  $1.5^\circ\text{C}$ . The local wall temperature was therefore got by averaging the data from the three relevant thermocouples to get  $T_{tc}$ , which was then corrected for depth from the plate surface,  $H_{tc}$ , through the one dimensional heat conduction equation, i.e.

$$T_w = T_{tc} - \frac{q_{eff} H_{tc}}{k} \quad (7)$$

The local of the single-phase heat transfer coefficients was obtained by separating the flow filed into cells. A typical two-dimensional unit cell at the location of

a thermocouple situated inside the copper test piece for the parallel test pieces is seen in the table below.

Table 2: Dimension for channel heat transfer analysis

Parallel channel test piece									
$W_w$	$W_{ch}$	$W_{cell}$	$L_{cell}$	$H_{w1}$	$H_{w2}$	$H_{w3}$	$H_{ch}$	$H_{tc}$	$H_{cell}$
mm	mm	mm	mm	mm	mm	mm	mm	mm	mm
1.0	1.0	2.0	2.0	10.0	5.0	5.0	1.0	1.5	21.0

$$Pr_f = \frac{c_{p,f} \mu_f}{k_f} \quad (8)$$

$$Re_f = \frac{G D_{ch}}{\mu_f} \quad (9)$$

In which ( $\mu_f$ ) is the liquid dynamic viscosity, ( $c_{p,f}$ ) the liquid specific heat capacity at constant pressure is and ( $G$ ) is the mass flux ( $\text{kg/m}^2\cdot\text{s}$ ),  $k_f$  thermal conductivity ( $\text{W/m}\cdot\text{K}$ ). The equation of the hydraulic diameter to the copper channel in the existence of the heat-transfer procedures, calculated by

$$D_h = \frac{4 H_c W_c}{2(W_c + H_c)} \quad (10)$$

#### 4. Evaluation of existing void fraction correlations for two phase

The applicability of the reviewed single-phase correlations to single-phase micro-channel flow is verified with the experimental and predictions data points. The Comparisons between predictions from the correlations and experimental data for parallel channel surface . The comparison include the root mean square error, (RMSE ), the coefficient of determination ( $R^2$  ), and mean absolute relative deviation ( MRE ) which defined as :-

$$RMSE = \sqrt{\frac{\sum_{i=1}^N [\alpha_{(i)measured} - \alpha_{(i)prediction}]^2}{N}} \quad (11)$$

$$R^2 = 1 - \frac{\sum_{i=1}^N [\alpha_{(i)measured} - \alpha_{(i)prediction}]^2}{\sum_{i=1}^N [\alpha_{(i)measured} - \alpha_{(i)average\ measured}]^2} \quad (12)$$

$$MRE = \frac{1}{N} \sum_{i=1}^N \frac{|\alpha_{(i)measured} - \alpha_{(i)prediction}|}{\alpha_{(i)measured}} \times 100\% \quad (13)$$

#### 5. Experimental Results and Discussion

Single-phase analysis, heat transfer coefficients measurements which were presented are analyzed in this paper. For the parallel channel surfaces, several popular macro- and micro-channel correlations for the empirical data were compared with the heat-transfer data. The variation of single phase heat transfer with heat flux is shown for the parallel channel surface as shown in Figure 5 .Heat flux is plotted in terms of  $T_h$  , for all mass fluxes and the relevance was Linear relationship. The difference between channel base wall temperature,  $T_w$  , and heater temperature , $T_h$ .

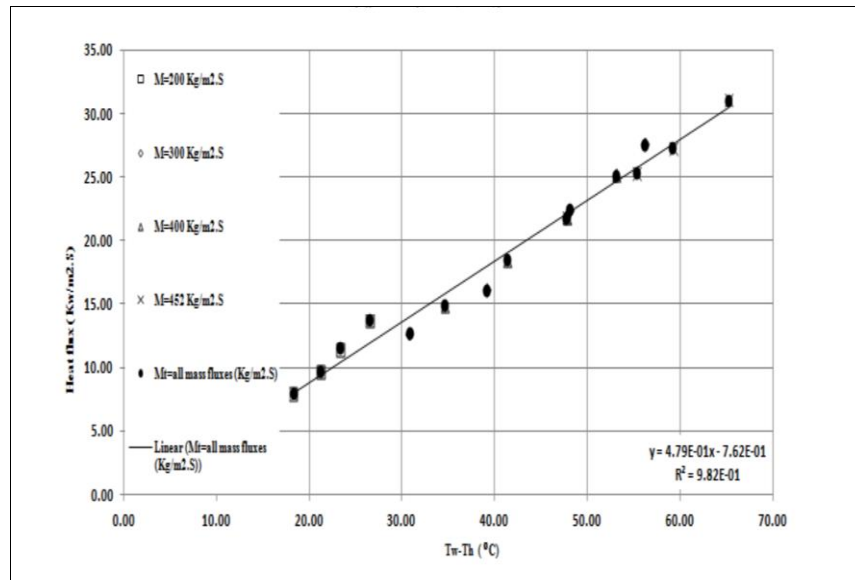


Fig.5 . Variation of effective heat flux with ( $T_h - T_w$ ) for Parallel channel

In Fig.6 gives the comparison of the prediction of the correlations with the empirical database. The inlet and outlet single-phase heat transfer are plotted for measured and prediction against experiment wall temperatures for 200, 300,400 and 425 kg/m<sup>2</sup> . RMSE, MRE and R<sup>2</sup> are

shown in plot. Besides, the predicting accuracy of the new correlation is also improved for two-phase flow in pipes. Therefore, the new correlation succeeds in accurately predicting the single-phase heat transfer coefficient of parallel channel heat sink

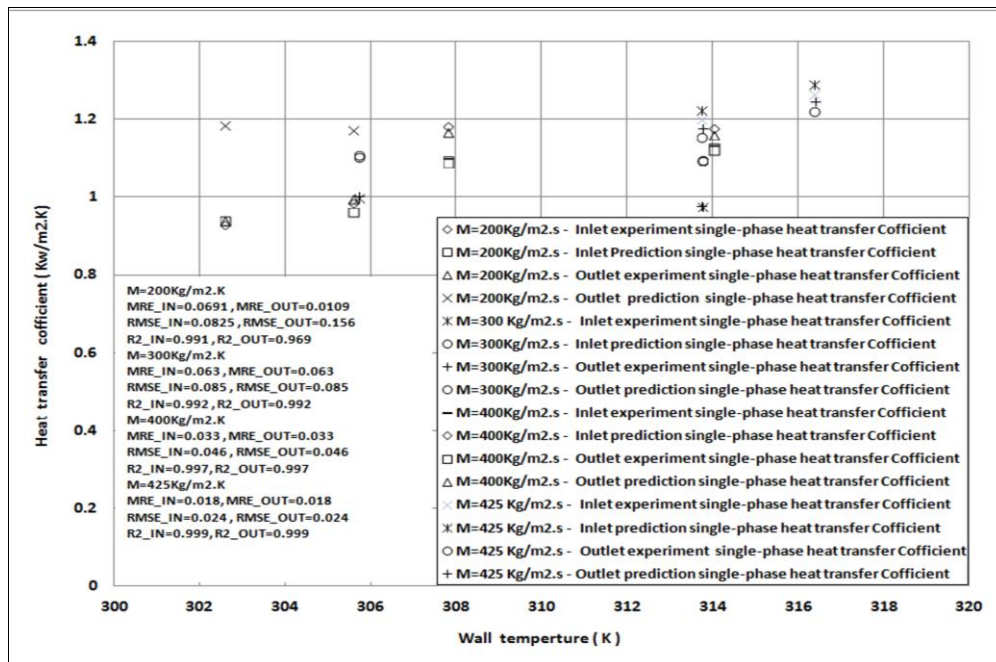


Fig.6. Variation of heat transfer coefficient with wall temperature

**Conclusions**

A 25 parallel channel test piece boiling R113, heat transfer has been obtained for them at atmospheric pressure. The channel's dimensions were fifty mm long by one mm square and by a constant heat-flux the channels were heated from below. The following conclusions can be drawn from this study:-

The data for single- phase heat transfer coefficients for R113 working fluid flow were calculated experimentally and compared with predictions data and the error were very small.

The heat flux distributions have deformities obtained from two causes. The first cause is because of end effects, and the second cause is because of the variation in liquid temperature, and heat transfers coefficient. To demonstrate the first cause, assume the channel contained a flow that was subjected to a uniform heat flux. To explain the Importance of the second effect, the heat conduction model outlined was solved for single phase flows.

All mass fluxes of the flows were laminar at outlet and inlet values in the test section.

The effective heat flux experiments data were very close to the predictions data for a range of mass fluxes.

Due to facilitate a comparison of the present results against the literature ,dimensionless thermal and hydrodynamic entrance lengths are found [11] .It is seen that the hydro dynamically developed and thermally developing conditions exist in the present experiments, using the criteria in the Ref.[11].

Acknowledgment

The author would like to thank my colleagues to their assistance to get these data.

**References**

- [1] G. Lazarek and S. Black, "Evaporative heat transfer, pressure drop and critical heat flux in a small vertical tube with R-113," International Journal of Heat and Mass Transfer, vol. 25, pp. 945-960, 1982.
- [2] D. Shiferaw, T. Karayiannis, and D. Kenning, "Flow boiling in a 1.1 mm tube with R134a: Experimental results and comparison with model," International Journal of Thermal Sciences, vol. 48, pp. 331-341, 2009.
- [3] W. Zhang, T. Hibiki, and K. Mishima, "Correlation for flow boiling heat transfer in mini-channels," International Journal of Heat and Mass Transfer, vol. 47, pp. 5749-5763, 2004.
- [4] S. G. Kandlikar and M. E. Steinke, "Flow boiling heat transfer coefficient in minichannels–correlation and trends," in Proceedings of the Twelfth International Heat Transfer Conference, 2002, pp. 785-790.
- [5] G. Fane and C. Phillips, "Effective Protection in Indonesia in 1987 1," Bulletin of Indonesian Economic Studies, vol. 27, pp. 105-125, 1991.
- [6] G. M. Harpole and J. E. Eninger, "Micro-channel heat exchanger optimization," in Semiconductor Thermal Measurement and Management Symposium, 1991. SEMI-THERM VII. Proceedings., Seventh Annual IEEE, 1991, pp. 59-63.
- [7] J. Knight, Institutions and social conflict: Cambridge University Press, 1992.

- [8] A. E. Bergles, J. H. Lienhard V, G. E. Kendall, and P. Griffith, "Boiling and evaporation in small diameter channels," *Heat Transfer Engineering*, vol. 24, pp. 18-40, 2003.
- [9] S. G. Kandlikar and H. R. Upadhye, "Extending the heat flux limit with enhanced microchannels in direct single-phase cooling of computer chips," in *Semiconductor Thermal Measurement and Management Symposium, 2005 IEEE Twenty First Annual IEEE*, 2005, pp. 8-15.
- [10] D. McNeil, A. Raeisi, P. Kew, and P. Bobbili, "A comparison of flow boiling heat-transfer in in-line mini pin fin and plane channel flows," *Applied thermal engineering*, vol. 30, pp. 2412-2425, 2010.
- [11] T. Chen and S. V. Garimella, "Effects of dissolved air on subcooled flow boiling of a dielectric coolant in a microchannel heat sink," *Journal of Electronic packaging*, vol. 128, pp. 398-404, 2006.